# Thermodynamics of Carbon in Liquid Manganese and Ferromanganese Alloys

EUI-JUN KIM, BYUNG-DON YOU, and JONG-JIN PAK

The thermodynamics of carbon in manganese and ferromanganese melts were studied to predict the refining limit of carbon during the decarburization of molten ferromanganese. The equilibrium carbon content in a Mn-C melt was determined by the C-CO equilibrium in the presence of pure solid MnO at 1673 to 1773 K. The activities of manganese and carbon in the Mn-C melt were then calculated from the experimental results, the equilibrium constant for the reaction, and the Gibbs–Duhem equation integrated by the Belton–Fruehan treatment. The standard free-energy change of carbon dissolution in the manganese melt was determined to be 41,700 − 59.6 $T$ J/g · atom, with the standard state taken as 1 wt pct carbon in solution. The effect of iron on the activity coefficient of carbon in ferromanganese was determined by measuring the carbon solubility in Mn-Fe melts. The first- and second-order interaction parameters between carbon and iron in ferromanganese melts were determined. The activity coefficient of carbon in the ferromanganese alloy melt can be expressed as

$$\log f_C = 0.0308 \text{ (pct C)} + 0.0136 \text{ (pct C)}^2 + 0.00867 \text{ (pct Fe)}$$

where the interaction parameters are independent of temperature in the temperature range of 1673 to 1773 K. The thermodynamic parameters determined in the present study could predict the equilibrium carbon content in the ferromanganese melt accurately for various melt compositions and CO partial pressures.

## I. INTRODUCTION

MANGANESE is an important element for iron and steel products. Ferromanganese alloys are generally used for alloying and as a deoxidizer in steelmaking. Recently, there has been a trend toward increased production of ultralow-carbon steel grades, and this situation increases the demand for low-carbon ferromanganese alloys. For the production of low-carbon ferromanganese alloys, the oxygen-inert gas blowing of molten high-carbon ferromanganese is an effective and economical process.[1–4] During the decarburization of ferromanganese, manganese oxidation also occurs. In order to establish an optimum decarburization process without excessive oxidation of manganese, it is important to know the thermodynamic behavior of carbon in manganese or ferromanganese liquid alloys.

There have been some experimental and theoretical studies on manganese activities in Mn-C[5–11] and Mn-Fe-C[10–16] liquid alloys. However, studies on carbon activities in these melts are very limited. Moreover, they treated iron as a solvent[13,15] and used interaction parameters for iron-based alloys in estimating the carbon activity in manganese-rich ferromanganese melts. Until now, the standard Gibbs free-energy change of carbon dissolution in liquid manganese and the activity coefficient of carbon in a manganese-rich ferromanganese melt have not been measured.

EUI-JUN KIM, formerly Graduate Student, Division of Materials and Chemical Engineering, Hanyang University, Ansan 425-791, Korea, is Research Associate with the Department of Materials Science and Engineering, Carnegie Melon University, Pittsburgh, PA 15213. BYUNG-DON YOU, Professor, is with the Division of Materials Science and Engineering, Inha University, Inchon 402-751, Korea. JONG-JIN PAK, Professor, is with the Division of Materials and Chemical Engineering, Hanyang University. Contact e-mail: jjpark@hanyang.ac.kr

Manuscript submitted September 18, 2001.

In the present study, the equilibrium carbon content of an Mn-C melt was determined by the C-CO equilibration in the presence of pure solid MnO in the temperature range of 1673 to 1773 K.

$$\text{MnO (s)} + \text{C (gr)} = \text{Mn (l)} + \text{CO (g)} \qquad [1]$$

From the equilibrium constant of reaction [1] and the Gibbs–Duhem relationship between manganese and carbon, the activity coefficients of these elements have been determined. The effect of iron on carbon in a ferromanganese melt was also determined by carbon-solubility measurements in Mn-Fe liquid alloys. The validity of the thermodynamic parameters determined in the present study was examined by measuring the equilibrium carbon content in ferromanganese melts of different Fe/Mn ratios under various CO partial pressures.

## II. EXPERIMENTAL

The experiment was carried out in an electric resistance furnace heated by SiC with a mullite reaction tube in the temperature range of 1673 to 1773 K, as shown in Figure 1. A detailed description is available elsewhere.[17] The alloys were made from electrolytic manganese (maximum of 0.018 wt pct N and 0.3 wt pct O), electrolytic iron (99.999 pct purity), and graphite powder (99.99 pct purity) by melting them in alumina crucible under an Ar atmosphere using a high-frequency induction furnace. Four grams of metallic charge and 0.4 g of MnO (99.5 pct purity) were placed in a high-purity alumina crucible (o.d.: 13 mm, i.d.: 9 mm, and height: 25 mm).

Five crucibles containing metallic charges with different carbon contents were suspended by Mo wire in the hot zone of the furnace. When the temperature had reached a desired value, Ar gas was switched to a mixture of Ar and CO. The gases were passed through columns of heated magnesium

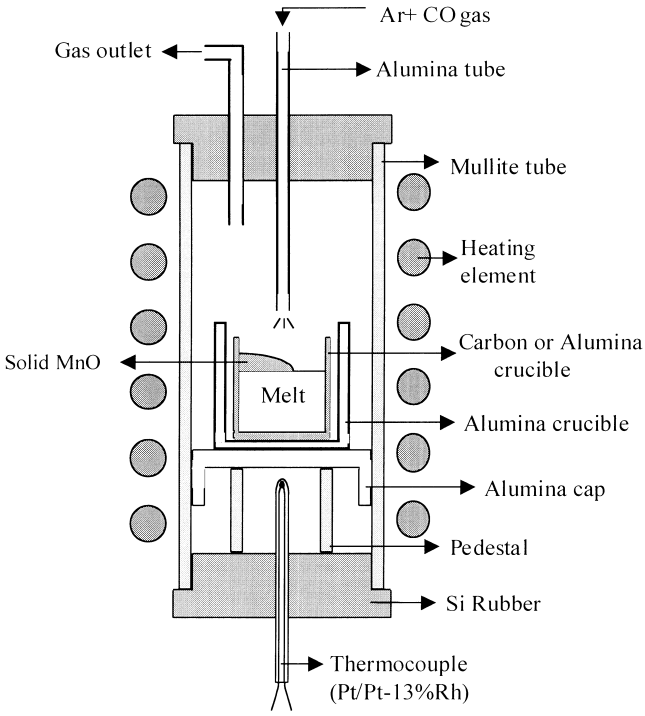


Fig. 1—A schematic diagram of the experimental apparatus.

turnings, Drierite, and magnesium perchlorate. The individual gas flow rate was controlled by a mass-flow controller (Curtis–Matheson, Model 8284). The mass-flow controller was calibrated at the exit of the gas inlet to within 1 pct, using a precision wet-test meter. The flow rate of mixed gas was in the range of 300 to 1000 mL/min, depending on gas composition.

In preliminary experiments, it was found that the time required for the C-CO equilibrium of the manganese melt in the presence of solid MnO was very long. Therefore, manganese alloys of different carbon contents were prepared, and, hence, the equilibrium could be approached from high and low carbon contents with respect to the equilibrium value. For carbon solubility measurements, Mn-Fe alloys of different compositions were melted in graphite crucibles under an Ar atmosphere.

After each experiment, the crucibles were pulled out and quenched rapidly in a He gas stream, followed by water quenching. Manganese oxide adhering to the top of the metal was removed and analyzed by the X-ray diffraction analysis for phase identification. The metallic sample was then crushed for the subsequent chemical analysis. Carbon was analyzed by the carbon/sulfur analyzer (LECO*, Model CS-300). The manganese and iron contents were measured by inductively coupled plasma-emission spectrometry (SPECTRO, Spectro Flame).

*LECO is a trademark of the LECO Corporation, St. Joseph, MI.

## III. RESULTS

### A. *Equilibrium Carbon Content in Manganese Melt under Various CO Pressures*

Table I and Figure 2 summarize the experimental results of equilibrium CO contents in a manganese melt under various CO pressures ($P_{CO}$) at 1673 to 1773 K. The melts were saturated with pure solid MnO, and it was confirmed by the X-ray diffraction analysis for manganese oxide adhered on the metal surface. The equilibrium carbon content decreases as $P_{CO}$ decreases, and the reduction of carbon content with decreasing $P_{CO}$ is significant at a low CO pressure range ($P_{CO} < \sim 20$ kPa). The increase of melt temperature significantly reduces the equilibrium carbon content. The present experimental data will be used to calculate carbon and manganese activities in Mn-C binary melts in Sections IV–A and IV–B.

### B. *Equilibrium Carbon Content in Ferromanganese Melt under Various CO Pressures*

The experimental results of equilibrium carbon contents in Mn-Fe melts under various $P_{CO}$ levels at 1723 K are summarized in Table II. The melts were also saturated with pure solid MnO. The equilibrium carbon content decreases with increasing iron content at a given $P_{CO}$. The present data will be used to check the validity of thermodynamic parameters of carbon in a ferromanganese melt in Sections IV–C and IV–D.

### C. *Carbon Solubility in Ferromanganese Melts*

In order to measure the effect of iron on carbon activity in Mn-Fe melts, the carbon solubility was measured as a function of iron content. Carbon saturation of the melt in a graphite crucible was achieved within 2 hours at 1673 K. The carbon solubility data are given in Table III and plotted in Figure 3 together with Ma *et al.*'s results.[16] The carbon-solubility data measured over a wide range of iron contents in the present study shows a good linear relationship with iron content in the temperature range of 1673 to 1773 K. The present data will be used to determine the effect of iron on the activity coefficient of carbon in ferromanganese melts in Section IV–C.

## IV. DISCUSSION

### A. *Activities in the Mn-C System*

Under the present experimental condition, carbon in manganese melt is equilibrated by the following reaction:

$$\text{MnO (s)} + \text{C (gr)} = \text{Mn (l)} + \text{CO (g)} \qquad [1]$$

$$\Delta G^{\circ}_T = 286{,}800 - 170.2\ T\ \text{J/mol}^{[18]}$$

$$K_{(1)} = \frac{a_{Mn} \cdot P_{CO}}{a_C} = \frac{X_{Mn} \cdot \gamma_{Mn} \cdot P_{CO}}{X_C \cdot \gamma_C} \qquad [2]$$

where $X_{Mn}$ and $X_C$ are the mole fractions, and $\gamma_{Mn}$ and $\gamma_C$ are the activity coefficients, of manganese and carbon in the Mn-C melt, respectively.

Manganese and carbon in the Mn-C melt will follow the Gibbs–Duhem relationship

$$X_C d \ln \gamma_C + X_{Mn} d \ln \gamma_{Mn} = 0 \qquad [3]$$

From the Belton–Fruehan treatment[19,20] of the Gibbs–Duhem equation, the activity coefficient of manganese in the Mn-C melt can be obtained from following equation:

**Table I. Experimental Results of C-CO Equilibration for Mn-C Melts**

| Number | Temperature | $P_{CO}$(kPa) | Time (h) | [Pct C] Initial | [Pct C] Final | [Pct C]$_{Average}$ |
|---|---|---|---|---|---|---|
| A1 | 1673 K | 2.03 | 27.5 | 1.61 | 1.38 ▼ | 1.25 |
| | | | | 0.65 | 1.11 ▲ | |
| A2 | | 3.04 | 24 | 2.14 | 1.82 ▼ | 1.65 |
| | | | | 1.18 | 1.47 ▲ | |
| A3 | | 5.07 | 24 | 2.94 | 2.24 ▼ | 2.35 |
| | | | | 1.61 | 2.47 ▲ | |
| A4 | | 7.09 | 26 | 3.60 | 3.33 ▼ | 3.10 |
| | | | | 2.14 | 2.86 ▲ | |
| A5 | | 10.13 | 24 | 4.09 | 3.97 ▼ | 3.88 |
| | | | | 3.60 | 3.78 ▲ | |
| A6 | | 20.27 | 23 | 5.26 | 4.82 ▼ | 4.69 |
| | | | | 4.09 | 4.55 ▲ | |
| A7 | | 40.53 | 24 | 6.07 | 5.58 ▼ | 5.50 |
| | | | | 5.26 | 5.43 ▲ | |
| A8 | | 60.80 | 24.5 | 6.29 | 5.97 ▼ | 6.04 |
| | | | | 5.66 | 6.11 ▲ | |
| A9 | | 101.33 | 25.5 | 7.24 | 6.59 ▼ | 6.57 |
| | | | | 6.29 | 6.55 ▲ | |
| B1 | 1723 K | 2.03 | 23 | 1.18 | 0.84 ▼ | 0.84 |
| | | | | 0.65 | 0.84 ▲ | |
| B2 | | 3.04 | 25 | 1.61 | 1.19 ▼ | 1.13 |
| | | | | 0.65 | 1.08 ▲ | |
| B3 | | 5.07 | 17 | 2.14 | 1.71 ▼ | 1.70 |
| | | | | 1.61 | 1.69 ▲ | |
| B4 | | 7.09 | 25 | 2.94 | 2.33 ▼ | 2.29 |
| | | | | 1.60 | 2.24 ▲ | |
| B5 | | 10.13 | 17 | 2.94 | 2.68 ▼ | 2.70 |
| | | | | 2.14 | 2.71 ▲ | |
| B6 | | 15.20 | 24 | 4.09 | 3.48 ▼ | 3.38 |
| | | | | 2.94 | 3.27 ▲ | |
| B7 | | 20.27 | 15.5 | 4.09 | 3.60 ▼ | 3.70 |
| | | | | 3.60 | 3.80 ▲ | |
| B8 | | 40.53 | 14 | 5.26 | 4.81 ▼ | 4.64 |
| | | | | 4.09 | 4.46 ▲ | |
| B9 | | 60.80 | 9 | 5.66 | 5.38 ▼ | 5.31 |
| | | | | 5.26 | 5.24 ▲ | |
| B10 | | 101.33 | 22 | 6.29 | 5.72 ▼ | 5.75 |
| | | | | 5.66 | 5.77 ▲ | |
| C1 | 1773 K | 2.03 | 22 | 0.65 | 0.54 ▼ | 0.50 |
| | | | | 0 | 0.45 ▲ | |
| C2 | | 3.04 | 24.5 | 1.18 | 0.75 ▼ | 0.73 |
| | | | | 0.65 | 0.72 ▲ | |
| C3 | | 5.07 | 24 | 1.61 | 1.09 ▼ | 1.05 |
| | | | | 1.18 | 1.00 ▲ | |
| C4 | | 10.13 | 21 | 2.14 | 1.82 ▼ | 1.84 |
| | | | | 1.61 | 1.86 ▲ | |
| C5 | | 15.20 | 27 | 2.94 | 2.59 ▼ | 2.54 |
| | | | | 2.14 | 2.49 ▲ | |
| C6 | | 20.27 | 15 | 2.94 | 2.88 ▼ | 2.85 |
| | | | | 2.14 | 2.82 ▲ | |
| C7 | | 30.40 | 24 | 4.09 | 3.49 ▼ | 3.74 |
| | | | | 2.94 | 3.98 ▲ | |
| C8 | | 40.53 | 25 | 5.26 | 4.36 ▼ | 4.35 |
| | | | | 4.09 | 4.34 ▲ | |
| C9 | | 60.80 | 25 | 5.26 | 4.76 ▼ | 4.82 |
| | | | | 4.09 | 4.87 ▲ | |
| C10 | | 101.33 | 19 | 5.66 | 5.36 ▼ | 5.32 |
| | | | | 5.26 | 5.29 ▲ | |

▼: High initial carbon content.
▲: Low initial carbon content.

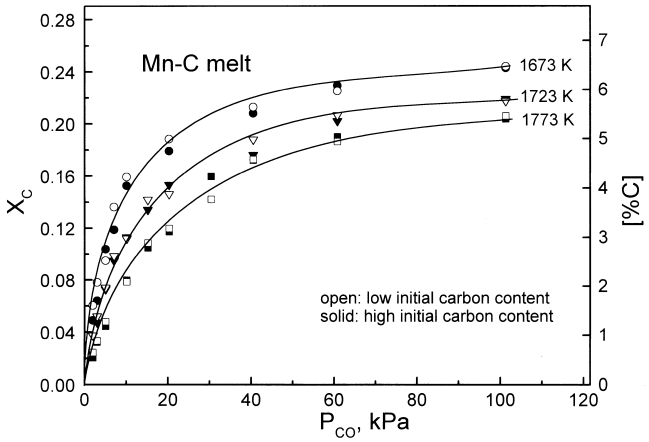


Fig. 2—The equilibrium carbon content in manganese melt at different $P_{CO}$ and melt temperatures.

**Table II. Experimental Result of C-CO Equilibrium for Mn-Fe-C Melts**

| Temperature | $P_{CO}$ (kPa) | Composition [Pct Fe] in Mn-Fe-C Alloys | Composition [Pct C] | |
|---|---|---|---|---|
| 1723 K | 2.03 | — | 0.842 | ▼ |
| | | — | 0.841 | ▲ |
| | | 6.64 | 0.633 | ▼ |
| | | 10.86 | 0.541 | ▲ |
| | | 12.67 | 0.568 | ▼ |
| | | 16.20 | 0.501 | ▲ |
| | | 20.13 | 0.494 | ▼ |
| | | 21.32 | 0.463 | ▲ |
| | | 24.48 | 0.413 | ▲ |
| | | 26.47 | 0.446 | ▼ |
| | | 33.71 | 0.344 | ▲ |
| | 3.04 | — | 1.185 | ▼ |
| | | — | 1.075 | ▲ |
| | | 16.37 | 0.769 | ▼ |
| | | 22.54 | 0.697 | ▼ |
| | 5.07 | — | 1.714 | ▼ |
| | | — | 1.685 | ▲ |
| | | 23.48 | 0.862 | ▲ |
| | | 23.98 | 0.978 | ▼ |
| | | 27.99 | 0.826 | ▲ |
| | | 29.38 | 0.927 | ▼ |
| | 10.13 | — | 2.682 | ▼ |
| | | — | 2.710 | ▲ |
| | | 21.06 | 1.822 | ▼ |
| | | 22.85 | 1.580 | ▲ |
| | | 25.93 | 1.687 | ▼ |
| | | 26.63 | 1.540 | ▲ |

▼:High initial carbon content.
▲:Low initial carbon content.

$$\log \gamma_{Mn} = -\int_{X_{Mn}}^{X_{Mn}=X_{Mn}} X_C d\left(\log\left(\frac{a_C}{a_{Mn}}\right) - \log\left(\frac{X_C}{X_{Mn}}\right)\right) \quad [4]$$

where the $a_C/a_{Mn}$ values can be determined from Eq. [2], and the $X_C/X_{Mn}$ values are measured equilibrium values at given CO partial pressures.

**Table III. Carbon Solubility in Mn-Fe Melts**

| Temperature | [Pct Fe] in Mn-Fe Alloys | [Pct C] |
|---|---|---|
| 1673 K | — | 7.71 |
| | 4.75 | 7.51 |
| | 9.70 | 7.37 |
| | 19.33 | 7.09 |
| | 23.31 | 6.93 |
| | 27.62 | 6.75 |
| 1723 K | — | 7.83 |
| | 4.81 | 7.62 |
| | 9.41 | 7.50 |
| | 18.40 | 7.20 |
| | 23.05 | 7.01 |
| | 27.58 | 6.95 |
| 1773 K | — | 7.91 |
| | 4.55 | 7.77 |
| | 9.52 | 7.60 |
| | 18.21 | 7.37 |
| | 23.19 | 7.24 |
| | 26.77 | 7.07 |

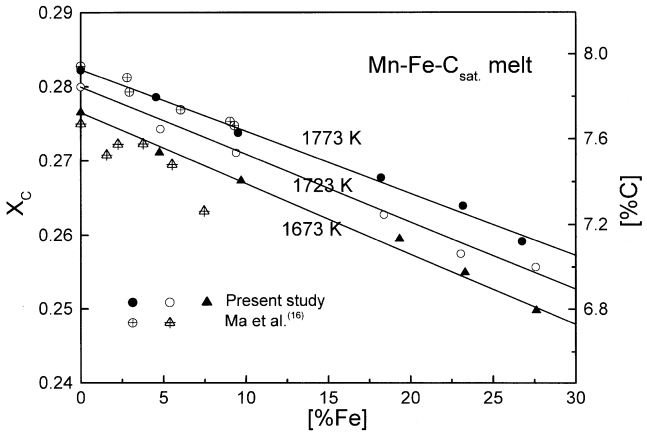


Fig. 3—The effect of iron on carbon solubility in Mn-Fe melts at different temperatures.

Therefore, the values of log $\gamma_{Mn}$ can be determined graphically as a function of melt composition, as illustrated in Figure 4. The activity coefficient of carbon, $\gamma_C$, can then be obtained from Eq. [2]. The activity coefficients of manganese and carbon in the Mn-C melt, determined as a function of melt composition in the temperature range of 1673 to 1773 K, are summarized in Table IV.

Figure 5 compares the $\gamma_{Mn}$ and $\gamma_C$ values in the Mn-C melt, determined in the present study at 1673 K, with previously reported data.[5,7,11] The manganese in the Mn-C melt shows nearly ideal solution behavior at low carbon contents up to $X_C \sim 0.1$ and shows a negative deviation at higher carbon contents. Carbon shows a negative deviation from ideal behavior up to $X_C \sim 0.19$ and a highly positive deviation at higher $X_C$ values up to its saturation. The activity coefficient of carbon at its saturation can be calculated from the following relationship:

$$\gamma_C^{sat} = \frac{1}{X_{C_{sat}}} \quad [5]$$

Tanaka[5] determined the manganese activity in Mn-C

alloys at 1673 K by the transportation method, which was equivalent to the vapor-pressure measurement. He measured the saturated vapor pressure of pure manganese and Mn-C melts using Ar gas as a carrier gas. In his work, the manganese activity showed a positive deviation from Raoult's law at carbon contents of $X_C < 0.17$ and showed a negative deviation at higher carbon contents. Katsnelson *et al.*[7] measured the equilibrium carbon content in molten Mn-C at 1628 K using a similar experimental technique to that of the present study. They obtained the expressions for activity coefficients of manganese and carbon as a function of carbon content in an Mn-C melt by the linear multiple regression analysis of their experimental data, using the interaction-parameter formalism developed by Lupis and Elliott.[21] These are shown as dashed-dotted lines in Figure 5. At their experimental temperature of 1628 K, however, the lowest equilibrium carbon content was 2.39 wt pct ($X_C = 0.101$) under a reduced $P_{CO}$ of 2.53 kPa.[7] Therefore, their data in the low-carbon range may not be accurate.

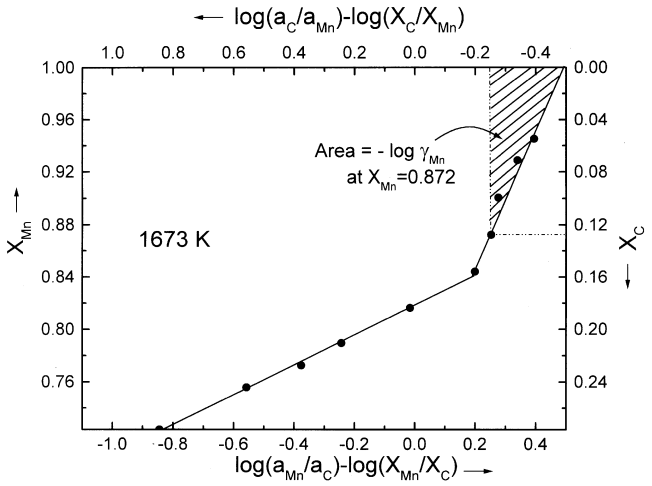


Fig. 4—The Belton–Fruehan plot for determining the Mn activity in the Mn-C melt at 1673 K.

Recently, Li and Morrise[11] evaluated the thermodynamics of a Mn-C melt using the unified interaction-parameter model developed by Bale and Pelton.[22,23] They expressed the activity coefficient of manganese as a function of carbon content by the linear multiple regression analysis of some selected experimental data of the Mn-C system.[5,7] They also derived the expression for the activity coefficient of carbon. The dotted lines in Figure 5 are their estimated expressions for the activity coefficients of manganese and carbon at 1673 K.

**Table IV. Activities of Manganese and Carbon in Mn-C Melts**

| Temperature | $X_C$ | $X_{Mn}$ | $a_C$ | $\gamma_C$ | $a_{Mn}$ | $\gamma_{Mn}$ |
|---|---|---|---|---|---|---|
| 1673 K | ~0 | 1 | — | 0.340 | 1 | 1 |
| | 0.055 | 0.945 | 0.022 | 0.401 | 0.941 | 0.995 |
| | 0.071 | 0.929 | 0.032 | 0.451 | 0.917 | 0.987 |
| | 0.099 | 0.901 | 0.051 | 0.515 | 0.877 | 0.974 |
| | 0.128 | 0.872 | 0.069 | 0.540 | 0.844 | 0.967 |
| | 0.156 | 0.844 | 0.094 | 0.601 | 0.803 | 0.951 |
| | 0.184 | 0.816 | 0.167 | 0.907 | 0.715 | 0.876 |
| | 0.211 | 0.789 | 0.291 | 1.383 | 0.624 | 0.791 |
| | 0.227 | 0.773 | 0.400 | 1.760 | 0.572 | 0.741 |
| | 0.244 | 0.756 | 0.592 | 2.425 | 0.508 | 0.672 |
| | 0.277 | 0.723 | 1 | 3.610 | 0.375 | 0.519 |
| 1723 K | ~0 | 1 | — | 0.304 | 1 | 1 |
| | 0.037 | 0.963 | 0.012 | 0.329 | 0.960 | 0.998 |
| | 0.050 | 0.950 | 0.018 | 0.366 | 0.946 | 0.996 |
| | 0.073 | 0.927 | 0.029 | 0.401 | 0.917 | 0.990 |
| | 0.097 | 0.903 | 0.040 | 0.412 | 0.888 | 0.983 |
| | 0.123 | 0.877 | 0.055 | 0.446 | 0.853 | 0.972 |
| | 0.138 | 0.862 | 0.078 | 0.564 | 0.810 | 0.939 |
| | 0.150 | 0.850 | 0.099 | 0.664 | 0.776 | 0.912 |
| | 0.182 | 0.818 | 0.176 | 0.964 | 0.685 | 0.837 |
| | 0.204 | 0.796 | 0.244 | 1.196 | 0.635 | 0.798 |
| | 0.218 | 0.782 | 0.366 | 1.679 | 0.572 | 0.731 |
| | 0.280 | 0.720 | 1 | 3.571 | 0.372 | 0.517 |
| 1773 K | ~0 | 1 | — | 0.287 | 1 | 1 |
| | 0.022 | 0.978 | 0.007 | 0.320 | 0.977 | 0.999 |
| | 0.033 | 0.967 | 0.011 | 0.323 | 0.965 | 0.998 |
| | 0.046 | 0.954 | 0.017 | 0.374 | 0.946 | 0.992 |
| | 0.079 | 0.921 | 0.033 | 0.418 | 0.906 | 0.984 |
| | 0.107 | 0.893 | 0.048 | 0.448 | 0.873 | 0.977 |
| | 0.118 | 0.882 | 0.062 | 0.521 | 0.845 | 0.959 |
| | 0.151 | 0.849 | 0.088 | 0.581 | 0.800 | 0.942 |
| | 0.172 | 0.828 | 0.112 | 0.648 | 0.765 | 0.925 |
| | 0.188 | 0.812 | 0.156 | 0.826 | 0.710 | 0.875 |
| | 0.205 | 0.795 | 0.235 | 1.146 | 0.643 | 0.808 |
| | 0.282 | 0.718 | 1 | 3.546 | 0.371 | 0.518 |

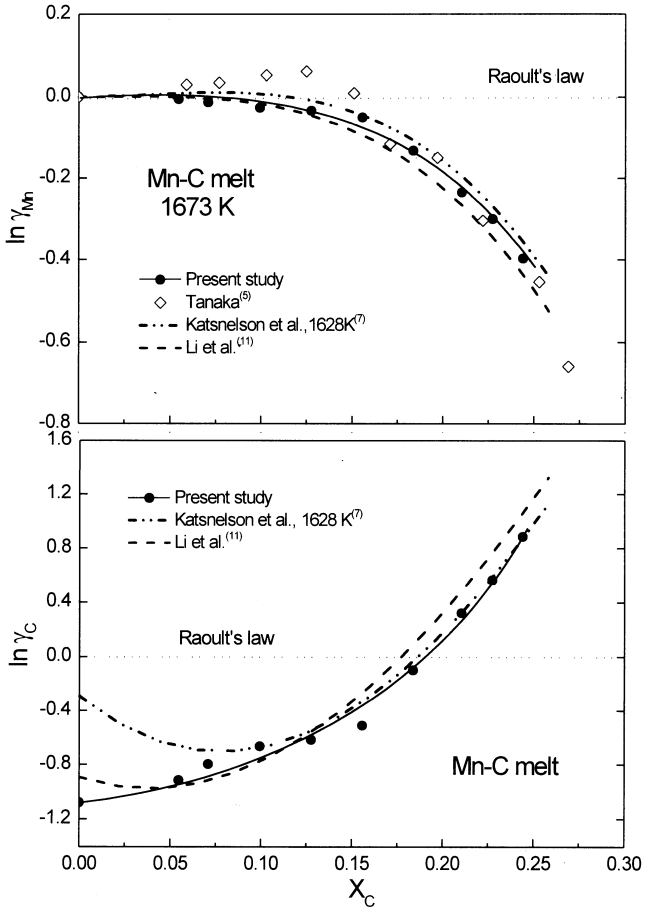


Fig. 5—Activity coefficients of manganese and carbon in the Mn-C melt.

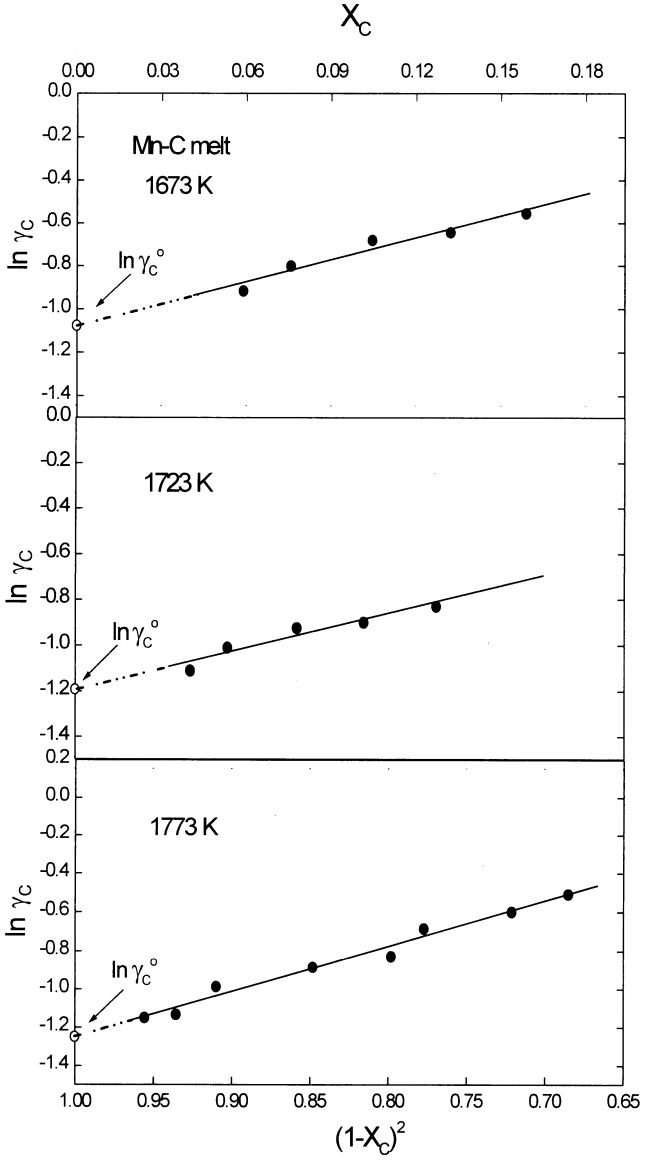


Fig. 6—The $\gamma_C$ values at the low carbon range in Mn-C melt at various temperatures.

### B. *Standard Gibbs Free-Energy Change of Carbon Dissolution in a Mn melt*

For the estimation of the standard Gibbs free-energy change of carbon dissolution in a manganese melt, the activity coefficient of carbon at infinite dilution ($\gamma_C^o$) should be known. The activity-coefficient data at the low-carbon range are plotted as a function of $(1 - X_C)^2$ in Figure 6. It shows a good linear relationship for the quadratic approximation of a regular solution.[24]

$$\ln \gamma_C = \alpha(1 - X_C)^2 \qquad [6]$$

where $\alpha$ is a constant.

Therefore, the $\gamma_C^o$ values at $X_C \sim 0$ can be obtained by the extrapolation method, and they are tabulated in Table IV. The temperature dependence of $\gamma_C^o$ in a manganese melt can be expressed as

$$\ln \gamma_C^o = -4.1 + \frac{5{,}040}{T} \qquad [7]$$

where $T$ is the temperature in Kelvin.

The standard Gibbs free-energy change of carbon dissolution in a manganese melt with the standard state of 1 wt pct solution ($\Delta G^o_{1\ wtpctlnMn}$) can be obtained by following formula:

$$C_{(gr)} = \underline{C}_{1\ wtpctlnMn} \qquad [8]$$

$$\Delta G^o_{1\ wtpctlnMn} = RT \ln \left( \gamma_C^o \frac{M_{Mn}}{100\ M_C} \right) \qquad [9]$$

$$= 41{,}700 - 59.6\ T\ \text{J/g} \cdot \text{atom}$$

where R is the universal gas constant (8.314 J/mole K), and $M_{Mn}$ and $M_C$ are the molar weights of manganese and carbon, respectively.

### C. *Henrian Activity Coefficient of Carbon in Ferromanganese Melts*

The standard state of 1 wt pct carbon in solution or the Henrian activity coefficient ($f_C$) is often more convenient to use. Therefore, the $f_C$ values in Mn-C melts can be determined by following relationship:

$$f_C = \frac{\gamma_C}{\gamma_C^o} \qquad [10]$$

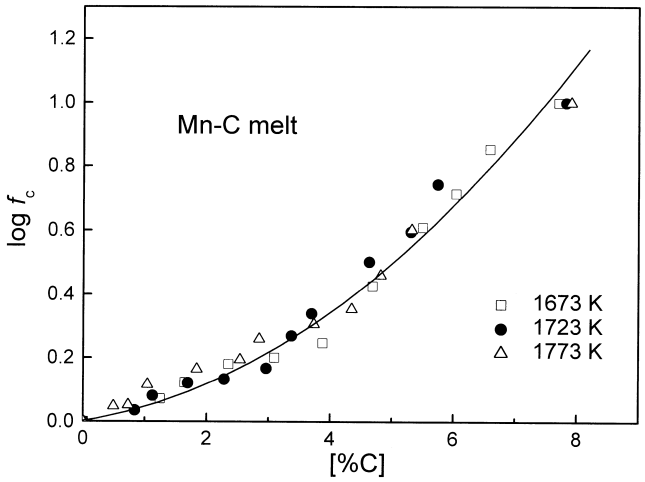


Fig. 7—Variation of $f_C$ values as a function of [pct C] in Mn-C melt.

Figure 7 shows the $f_C$ values plotted *vs* carbon content in weight percent at different temperatures. The activity coefficient of carbon increases sharply with increasing carbon content. For a carbon-saturated melt, the $f_C$ value is nearly 10. However, the temperature dependence of the activity coefficient is not significant. The relationship can be analytically expressed using the generalized interaction-coefficient model developed by Lupis and Elliott.[21]

$$\log f_C = e_C^C\,(\text{pct C}) + \gamma_C^C\,(\text{pct C})^2 \qquad [11]$$

where the values of $e_C^C$ and $\gamma_C^C$ are determined as 0.0308 and 0.0136, respectively.

In order to establish the carbon activity in a ferromanganese melt, the effect of iron on carbon in the manganese melt should be known. The activity coefficient of carbon in a ferromanganese melt can be expressed as

$$\begin{aligned}\log f_C = {} & e_C^C\,(\text{pct C}) + \gamma_C^C\,(\text{pct C})^2 \\ & + e_C^{Fe}\,(\text{pct Fe}) + \gamma_C^{Fe}\,(\text{pct Fe})^2 \\ & + \gamma_C^{Fe,C}\,(\text{pct Fe})(\text{pct C})\end{aligned} \qquad [12]$$

In order to determine the values of $e_C^{Fe}$, $\gamma_C^{Fe}$, and $\gamma_C^{Fe,C}$ in Eq. [12], the carbon-solubility data for Mn-Fe melts, shown in Table III, can be used. The Henrian activity coefficient at carbon saturation ($f_C^{sat}$) can be also expressed as

$$\begin{aligned}\log f_C^{sat} &= \log \frac{\gamma_C^{sat}}{\gamma_C^o} \\ &= e_C^C\,(\text{pct C})_{sat} + \gamma_C^C\,(\text{pct C})_{sat}^2 + e_C^{Fe}\,(\text{pct Fe}) \\ &\quad + \gamma_C^{Fe}\,(\text{pct Fe})^2 + \gamma_C^{Fe,C}\,(\text{pct Fe})(\text{pct C})_{sat}\end{aligned} \qquad [13]$$

where the $\gamma_C^{sat}$ values at carbon saturation can be obtained using Eq. [5], $(\text{pct C})_{sat}$ is the carbon content at saturation, and the values of $e_C^C$ and $\gamma_C^C$ were determined previously.

Equation [13] can then be rearranged as

$$\begin{aligned}\log f_C^{sat} - e_C^C\,(\text{pct C})_{sat} - \gamma_C^C\,(\text{pct C})_{sat}^2 \\ = e_C^{Fe}\,(\text{pct Fe}) + \gamma_C^{Fe}\,(\text{pct Fe})^2 \\ + \gamma_C^{Fe,C}\,(\text{pct Fe})(\text{pct C})_{sat}\end{aligned} \qquad [14]$$

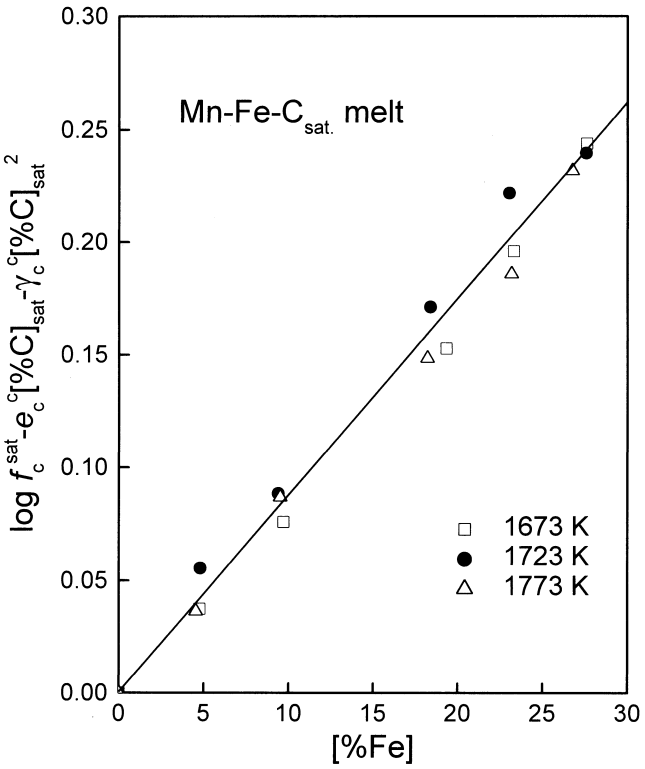


Fig. 8—Relation between $\log f_C^{sat} - e_C^C\,[\text{pct C}]_{sat} - \gamma_C^C\,[\text{pct C}]_{sat}^2$ and [pct Fe] in Mn-Fe-$C_{sal}$ melts.

Figure 8 shows the relationship between the left-hand side of Eq. [14] and iron content in carbon-saturated Mn-Fe melts. It can be seen that a linear relationship is obtained over a wide range of iron contents. The temperature dependence of the relationship is not significant. Therefore, only the first-order interaction parameter of iron ($e_C^{Fe}$) can be considered, and the second-order terms can be neglected. The $e_C^{Fe}$ value is determined to be 0.00867 by the linear regression analysis.

Therefore, the Henrian activity coefficient of carbon in a ferromanganese melt can be expressed by Eq. [15] in the temperature range of 1673 to 1773 K.

$$\begin{aligned}\log f_C = {} & 0.0308\,(\text{pct C}) + 0.0136\,(\text{pct C})^2 \\ & + 0.00867\,(\text{pct Fe})\end{aligned} \qquad [15]$$

### D. *Equilibrium Carbon Content in the Ferromanganese Melt*

In order to check the validity of Eq. [15] where the $e_C^{Fe}$ value was determined from the carbon-solubility data for Mn-Fe melts, the equilibrium carbon content in the ferromanganese melt was measured as a function of iron content under various CO partial pressures at 1723 K. The experimental data are summarized in Table II and shown in Figure 9. In these experiments, the equilibrium was approached from both sides with respect to the equilibrium carbon contents, as discussed earlier.

The equilibrium carbon content can be also calculated using the thermodynamic data for the following reaction equilibrium:

$$\text{MnO (s)} + \underline{\text{C}}_{(1\ \text{wtpctlnMn})} = \text{Mn (l)} + \text{CO (g)} \qquad [16]$$

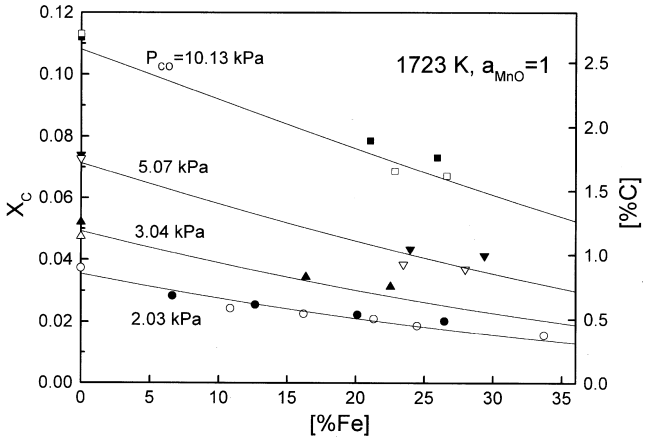


Fig. 9—Correlation between the measured and calculated values of equilibrium carbon content in the Mn-Fe-C melt.

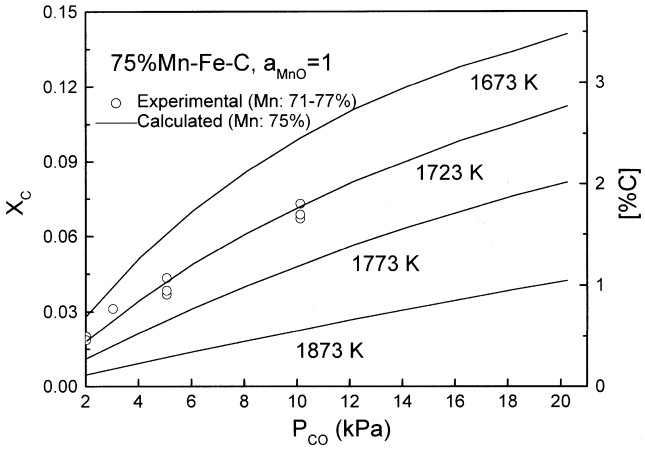


Fig. 10—The refining limit of carbon in the ferromanganese melt as a function of melt temperature and $P_{CO}$.

$$\Delta G^{\circ}_T = 245{,}100 - 110.6\ T\ \text{J/g} \cdot \text{atom}^{[18,\text{present work}]}$$

$$K^{[16]} = \frac{a_{Mn} \cdot P_{CO}}{a_{MnO} \cdot f_C\ (\text{pct C})} \qquad [17]$$

where $f_C$ can be calculated using Eq. [15] as a function of melt composition.

In the present experimental condition, the slag was virtually saturated with pure solid MnO, and, hence, $a_{MnO}$ can be considered as unity. The activity of manganese in a manganese-rich ferromanganese melt can be considered as $X_{Mn}$ at relatively low carbon contents. Enokido *et al.*[13] determined the manganese activity in Fe-Mn-C melts containing 15 to 40 at. pct Mn by equilibrating with Ag-Mn melts of known manganese activity. They found that the $\gamma_{Mn}$ value in a Fe-Mn-C melt was nearly 1 at carbon contents up to $X_C \sim 0.1$.

The solid lines shown in Figure 9 are the calculated equilibrium carbon contents as a function of iron content at different $P_{CO}$ values at 1723 K. The correlation between the measured and the calculated values shows an almost perfect agreement, indicating that the thermodynamic parameters of carbon determined in the present study are well established.

Using the thermodynamic parameters of carbon, the refining limit of carbon in a ferromanganese melt can be predicted as a function of the melt temperature and $P_{CO}$. The $P_{CO}$ value in the decarburization process can be estimated from the mixing ratio of oxygen and Ar in the gas mixture blown into the melt.

$$P_{CO} = \frac{2\ Q_{O_2}}{(2\ Q_{O_2} + Q_{Ar})} \cdot P_{hubble} \qquad [18]$$

where $Q_{O_2}$ and $Q_{Ar}$ are the flow rates of oxygen and Ar, respectively, and $P_{bubble}$ is the absolute pressure in rising gas bubbles in the melt.

Figure 10 shows the equilibrium carbon content obtainable during the final stage of oxygen-inert gas blowing. The measured equilibrium carbon contents in ferromanganese-type melts (71 to 77 pct Mn) at 1723 K are also shown in the figure. It can be seen that a high melt temperature and reduced $P_{CO}$ are very effective in lowering the refining limit of carbon in a ferromanganese melt. The final carbon content below 0.5 wt pct can be obtained at a $P_{CO}$ level of ~10 kPa at a melt temperature of 1873 K.

## V. CONCLUSIONS

The equilibrium carbon content in a Mn-C melt has been determined by the C-CO equilibrium in the presence of pure solid MnO at 1673 to 1773 K. The manganese and carbon activities were calculated from the equilibrium constant of the reaction and the Gibbs–Duhem relationship. The standard free-energy change for the carbon dissolution in a manganese melt, $\Delta G^{\circ}_{1\ \text{wt pct in Mn}}$, has been determined to be 41,700 − 59.6 $T$ J/g·atom. The effect of iron content on carbon activity in a ferromanganese melt was also determined from the carbon-solubility data in Mn-Fe melts. Using Lupis and Elliott's generalized interaction-coefficient formalism, the Henrian activity coefficient of carbon in ferromanganese melts could be well described as a function of melt composition as

$$\log f_C = 0.0308\ (\text{pct C}) + 0.0136\ (\text{pct C})^2 + 0.00867\ (\text{pct Fe})$$

where the interaction parameters are independent of temperature in the temperature range of 1673 to 1773 K. The present model accurately predicted the equilibrium carbon content in a ferromanganese melt under various operational conditions.

## REFERENCES


1. D.S. Kozak and L.R. Matricardi: *Iron Steelmaker*, 1981, vol. 8, pp. 28-31.
2. E. Schürmann, A. Ender, E. Hoffken, H. Litterscheld, and C.H. Schütz: *Stahl Eisen.*, 1993, vol. 113, pp. 77-82.
3. B.D. You, K.Y. Park, J.J. Pak, and J.W. Han: *Met. Mater.*, 1999, vol. 5, pp. 395-99.
4. B.D. You, J.W. Han, and J.J. Pak: *Steel Res.*, 2000, vol. 71, pp. 22-26.
5. A. Tanaka: *Trans. JIM*, 1979, vol. 20, pp. 516-22.
6. R. Gee and T. Rosenqvist: *Scand. J. Metall.*, 1976, vol. 5, pp. 57-62.
7. A. Katsnelson, F. Tsukihashi, and N. Sano: *Iron Steel Inst. Jpn. Int.*, 1993, vol. 33, pp. 1045-48.
8. J.O. Edström and C. Liu: "Dephosphorization of Ferromanganese Melts. Part 1, Theoretical Considerations," *China-Sweden Symp.*, Stockholm, May 1992, p. 15.
9. W. Huang: *Scand. J. Metall.*, 1990, vol. 19, pp. 26-32.
10. Y.E. Lee and J.H. Downing: *Can. Metall. Q.*, 1980, vol. 19, pp. 315-22.

11. H. Li and A. Morris: *Metall. Mater. Trans. B*, 1997, vol. 28B, pp. 553-62.
12. A. Tanaka: *Trans. JIM*, 1980, vol. 21, pp. 27-33.
13. H. Enokido, A. Moro-oka, and E. Ichise: *Tetsu-to-Hagané*, 1995, vol. 81, pp. 619-24.
14. G.W. Healy: *Proc. Int. Symp. on Ferrous and Nonferrous Alloy Process*, R.A. Bergman, ed., Pergaman Press, Elmsford, NY, 1990, pp. 97-108.
15. W. Dresler: *Trans. Inst. Min. Metall., Sec. C*, 1989, vol. 98, pp. 61-67.
16. Z. Ma, R. Ni, and W. Cheng: *Steel Res.*, 1991, vol. 62, pp. 481-87.
17. E.J. Kim, B.D. You, and J.J. Pak: *Metall. Mater. Trans. B*, 2001, vol. 32B, pp. 659-68.
18. E.T. Turkdogan: *Physical Chemistry of High Temperature Technology*, Academic Press, New York, NY, 1980.
19. G.R. Belton and R.J. Fruehan: *J. Phys. Chem.*, vol. 71, pp. 1403-1409.
20. D.R. Gaskell: *Introduction to Metallurgical Thermodynamics*, 2nd ed., McGraw-Hill Company, New York, NY, 1981.
21. C.H.P. Lupis and J.F. Elliott: *Acta Metall.*, 1966, vol. 14, pp. 529-38.
22. A.D. Pelton and C.W. Bale: *Metall. Trans. A*, 1986, vol. 17A, pp. 1211-15.
23. C.W. Bale and A.D. Pelton: *Metall. Trans. A*, 1990, vol. 21A, pp. 1997-2002.
24. A.W. Porter: *Trans. Faraday Soc.*, 1921, vol. 16, pp. 336-45.